An inactive receptor-G protein complex maintains the dynamic range of agonist-induced signaling

Wonjo Jang[a], C. Elizabeth Adams[a], Heng Liu[b], Cheng Zhang[b], Finn Olav Levy[c], Kjetil Wessel Andressen[c], and Nevin A. Lambert[a,1]

[a]Department of Pharmacology and Toxicology, Medical College of Georgia, Augusta University, Augusta, GA 30912; [b]Department of Pharmacology and Chemical Biology, School of Medicine, University of Pittsburgh, Pittsburgh, PA 15261; and [c]Department of Pharmacology, Institute of Clinical Medicine, University of Oslo and Oslo University Hospital, 0188 Oslo, Norway

Edited by Robert J. Lefkowitz, Howard Hughes Medical Institute, Durham, NC, and approved October 13, 2020 (received for review May 27, 2020)

Agonist binding promotes activation of G protein-coupled receptors (GPCRs) and association of active receptors with G protein heterotrimers. The resulting active-state ternary complex is the basis for conventional stimulus-response coupling. Although GPCRs can also associate with G proteins before agonist binding, the impact of such preassociated complexes on agonist-induced signaling is poorly understood. Here we show that preassociation of 5-HT_7 serotonin receptors with G_s heterotrimers is necessary for agonist-induced signaling. 5-HT_7 receptors in their inactive state associate with G_s, as these complexes are stabilized by inverse agonists and receptor mutations that favor the inactive state. Inactive-state 5-HT_7–G_s complexes dissociate in response to agonists, allowing the formation of conventional agonist–5-HT_7–G_s ternary complexes and subsequent G_s activation. Inactive-state 5-HT_7–G_s complexes are required for the full dynamic range of agonist-induced signaling, as 5-HT_7 receptors spontaneously activate G_s variants that cannot form inactive-state complexes. Therefore, agonist-induced signaling in this system involves two distinct receptor-G protein complexes, a conventional ternary complex that activates G proteins and an inverse-coupled binary complex that maintains the inactive state when agonist is not present.

GPCR | G protein | ternary complex | precoupling | serotonin

G protein-coupled receptors (GPCRs) transduce a wide variety of physiological signals and are targeted by a substantial fraction of all therapeutic drugs (1). GPCRs are conformationally dynamic and transition between inactive and active states, the latter being capable of interacting with and activating heterotrimeric G proteins (2). Although some level of constitutive activity is common, the conformational equilibrium "setpoint" usually favors the inactive state of the receptor, thus keeping the system turned off and ready to respond to agonists. Agonist binding stabilizes active conformations and promotes the formation of transient active-state ternary agonist-receptor-G protein complexes (3). This positive allosteric interaction between agonist and G protein binding is the hallmark of conventional GPCR coupling. Receptor-G protein complexes that form before agonist binding have also been described (4–8) and are generally thought of as a means to promote rapid or specific signaling after agonist binding. However, the properties and functional significance of such "preassociated" complexes are largely unknown, and inactive receptor conformations are generally considered unable to interact with G proteins. Here we show that unliganded 5-HT_7 serotonin receptors form complexes with G_s heterotrimers, and that these complexes help maintain the receptor in an inactive state. Agonist binding leads to dissociation of inactive-state 5-HT_7–G_s complexes, which in turn allows increased formation of active-state 5-HT_7–G_s complexes and G protein activation. Thus, a negative allosteric interaction between agonist and G protein binding is required for the full sensitivity of these receptors to serotonin.

Results

Agonist Activation Leads to Net Dissociation of Preassociated 5-HT_7–G_s Complexes. 5-HT_7 serotonin receptors activate G_s heterotrimers to stimulate adenylyl cyclase (AC) (9, 10), and previous work has shown that these receptors form complexes with G_s before agonist binding (11–13). We set out to determine the impact of 5-HT_7–G_s preassociation on agonist-induced activation of G_s and signaling. Consistent with previous fluorescence studies (13), stimulation with serotonin (5-HT; Fig. 1*A*) decreased bioluminescence resonance energy transfer (BRET) between labeled 5-HT_7 receptors and G_s heterotrimers. This is unusual, as energy transfer between GPCRs and G proteins usually increases in response to agonist activation (14) owing to formation of active-state receptor-G protein complexes (e.g., β_2 adrenergic receptors [β_2AR]) (Fig. 1*A*).

To determine whether 5-HT prompted dissociation of 5-HT_7–G_s complexes or a change in complex conformation, we took a luciferase complementation approach (15) that reports protein association and dissociation more directly than energy transfer. We fused a small fragment of luciferase (SmBit) to the C terminus of each receptor and a large fragment of luciferase (LgBit) to the N terminus of $G\gamma_2$ and expressed these proteins with $G\alpha_s$ and $G\beta_1$. Luciferase activity decreased on stimulation of 5-HT_7-SmBit but increased on stimulation of β_2AR-SmBit (Fig. 1*B*), consistent with net dissociation and association of receptor-G_s complexes, respectively. Changes in luminescence occurred more slowly than corresponding changes in BRET, presumably due to the slow kinetics of luciferase fragment association and dissociation (15). In these experiments, $G\beta\gamma$ was labeled instead of the $G\alpha_s$ subunit so

Significance

G protein-coupled receptors (GPCRs) are targeted by a large fraction of approved drugs and regulate many important cellular processes. Conventional signaling by GPCRs is triggered when agonist-activated receptors associate with heterotrimeric G proteins. We found that serotonin 5-HT_7 receptors couple to G_s proteins in an unconventional manner, in which agonist binding instead promotes dissociation of preexisting inactive 5-HT_7–G_s complexes. Therefore, agonists can initiate signaling via two distinct mechanisms, by promoting the association of active receptors and G proteins and by promoting dissociation of inactive receptors and G proteins.

Author contributions: W.J., C.Z., and N.A.L. designed research; W.J., C.E.A., H.L., K.W.A., and N.A.L. performed research; W.J., C.Z., K.W.A., and N.A.L. analyzed data; and W.J., F.O.L., K.W.A., and N.A.L. wrote the paper.

The authors declare no competing interest.

This article is a PNAS Direct Submission.

[1]To whom correspondence may be addressed. Email: NELAMBERT@augusta.edu.

This article contains supporting information online at https://www.pnas.org/lookup/suppl/doi:10.1073/pnas.2010801117/-/DCSupplemental.

First published November 16, 2020.

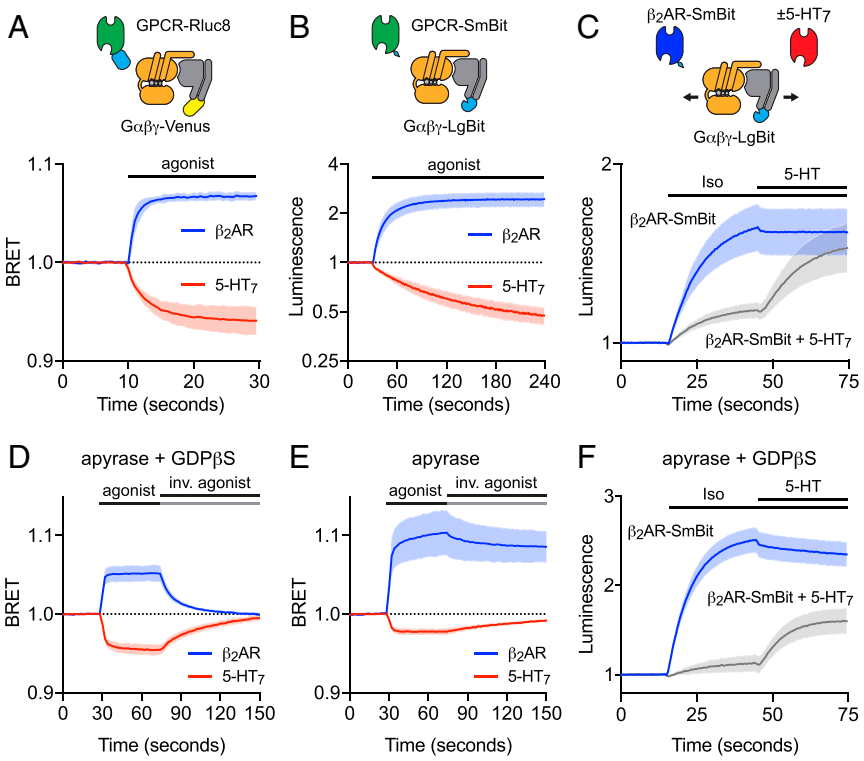

Fig. 1. 5-HT$_7$–G$_s$ complexes dissociate in response to agonist stimulation. (*A*) In intact cells, BRET between 5-HT$_7$-Rluc8 and Gα$_s$βγ-Venus decreases in response to agonist (5-hydroxytryptamine; 10 μM; n = 20), whereas BRET between β$_2$AR-Rluc8 and Gα$_s$βγ-Venus increases in response to agonist (isoproterenol; 10 μM; n = 20). (*B*) Luciferase complementation between 5-HT$_7$-SmBit and Gα$_s$βγ-LgBit decreases in response to agonist (5-HT; n = 20), whereas luciferase complementation between β$_2$AR-SmBit and Gα$_s$βγ-LgBit increases in response to agonist (Iso; n = 16). (*C*) Iso-induced luciferase complementation between β$_2$AR-SmBit and Gα$_s$βγ-LgBit is blunted when 5-HT$_7$ receptors are coexpressed, and this is alleviated by stimulation with 5-HT (n = 14). (*D* and *E*) Similar to *A*, (*F*) similar to *C*, but in permeabilized cells under conditions in which G$_s$ cannot be activated, treated with either apyrase and 100 μM GDPβS (*D* and *F*; n = 16 and 22) or apyrase alone (*E*, n = 8 to 12). The responses shown in *D* and *E* recovered on the addition of inverse agonists (MT and ICI-118,551; 10 μM). Traces represent mean ± SD.

as to minimize interference with normal G protein function and receptor-G protein interactions. This left open the possibility that Gα$_s$ subunits remained associated with 5-HT$_7$ receptors after agonist activation. To address this, we used a competition strategy in which luciferase complementation between β$_2$AR receptors and G$_s$ heterotrimers was monitored in the presence and absence of unlabeled 5-HT$_7$ receptors. Expression of 5-HT$_7$ receptors inhibited agonist-induced association of β$_2$AR-SmBit and Gαβγ-LgBit, consistent with sequestration of G$_s$ by 5-HT$_7$ (12). This inhibition was relieved by stimulation with 5-HT (Fig. 1*C*), indicating that agonist activation of 5-HT$_7$ made more G$_s$ heterotrimers available to other GPCRs.

We next tested the hypothesis that preassociated 5-HT$_7$-G$_s$ complexes dissociate in response to agonist because G$_s$ binds GTP and becomes activated. Accordingly, we repeated the above experiments in permeabilized cells in the absence of GTP. To eliminate the possibility that residual GTP was present, we used apyrase to hydrolyze endogenous nucleotides and replaced them with either the hydrolysis-resistant analog GDPβS or no nucleotide at all. Agonist-induced BRET changes were retained under these conditions (Fig. 1 *D* and *E*), although the 5-HT–induced decrease was blunted in the absence of any nucleotide. Since active-state agonist-GPCR-G protein complexes are stabilized in the absence of guanine nucleotides (2, 16), it is likely that 5-HT promoted both the dissociation of preassociated 5-HT$_7$–G$_s$ complexes and the formation of conventional active-state complexes, resulting in a smaller net dissociation when nucleotides are absent. In contrast, the agonist-induced increase in BRET between β$_2$AR and G$_s$ was larger in the absence of nucleotides (Fig. 1*E*), consistent with only active-state complexes. Sequestration and agonist-induced release of G$_s$ heterotrimers by 5-HT$_7$ receptors was also observed in the absence of GTP (Fig. 1*F*). These results indicate that agonist-induced dissociation of preassociated 5-HT$_7$–G$_s$ complexes does not require G$_s$ activation.

5-HT$_7$ Receptors in Their Inactive State Preassociate with G$_s$. GPCRs are conformationally dynamic and can sample intermediate states between the fully inactive and active states. To assess the conformational state of 5-HT$_7$ receptors when preassociated with G$_s$ heterotrimers, we first applied inverse agonists, which stabilize the inactive state of GPCRs. Several 5-HT$_7$ inverse agonists produced small but significant increases in BRET between 5-HT$_7$ receptors and G$_s$ heterotrimers (Fig. 2*A*). Similarly, in pull-down assays, we also found that detergent-solubilized 5-HT$_7$ receptors retained G$_s$ more efficiently in the presence of an inverse agonist (methiothepin [MT]) than in the presence of an agonist (5-HT) if GDP was present, whereas this was not the case for solubilized β$_2$AR (*SI Appendix*, Fig. S1). These results with inverse agonists suggest that 5-HT$_7$ receptors in their inactive state associate with G$_s$.

To further test this idea, we introduced mutations to produce constitutively inactive (CIM) and active (CAM) 5-HT$_7$ receptors. For CIM receptors, residues F336$^{6\times44}$ and N380$^{7\times49}$ were mutated individually to positively charged residues, in both cases to promote interactions with D127$^{2\times50}$ that stabilize the inactive state. To produce a CAM receptor residue, L173$^{3\times43}$ was mutated to alanine to weaken hydrophobic interactions with residues in transmembrane helix 6 and promote activation. We have previously shown that both of these CIM receptors fail to support the activation of G$_s$ and AC,

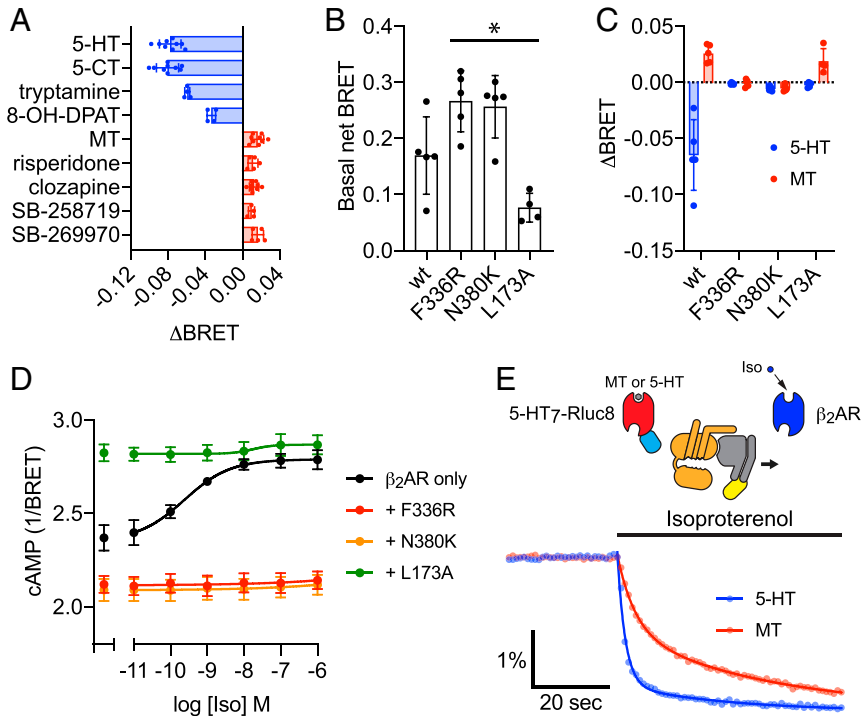

Fig. 2. Inactive-state 5-HT$_7$ receptors form complexes with and sequester G$_s$ heterotrimers. (*A*) Agonists (blue) decrease and inverse agonists (red) increase BRET between 5-HT$_7$-Rluc8 and Gα$_s$βγ-Venus. BRET changes relative to vehicle controls (ΔBRET) were all significantly different from 0; $P < 0.01$, one-sample *t* test, $n = 4$ to 9. All ligands were tested at 10 μM with the exception of tryptamine and SB-258719 (100 μM). (*B*) Introduction of inactivating mutations in 5-HT$_7$ (N380K and F336R) increases basal BRET, whereas introduction of an activating mutation (L173A) decreases basal BRET between 5-HT$_7$-Rluc8 and Gα$_s$βγ-Venus. Data are mean ± SD; $n = 4$ to 5. $P < 0.05$, one-way ANOVA (Dunnett's test). (*C*) Inactivating and activating mutations prevent the 5-HT–induced decrease in BRET, whereas only inactivating mutations prevent the MT-induced increase in BRET between 5-HT$_7$-Rluc8 and Gα$_s$βγ-Venus ($n = 4$ to 5). (*D*) Inactive mutant 5-HT$_7$ receptors abolish β$_2$AR receptor-mediated activation of AC, whereas active mutant 5-HT$_7$ receptors constitutively activate AC. cAMP was measured in intact cells using an EPAC-based BRET sensor that indicates increases in cAMP with lower BRET. Data are mean ± SEM; $n = 5$. (*E*) Activation of unlabeled β$_2$AR in the absence of nucleotides decreases BRET between 5-HT$_7$-Rluc8 and Gα$_s$βγ-Venus, and the decrease occurs more slowly when the inverse agonist MT is present than when the agonist 5-HT is present (both at 10 μM). Traces represent normalized BRET and are the average of 24 (MT) or 28 (5-HT) replicates from three independent experiments, superimposed with fits to a two-component exponential decay. Fitted parameters are provided in *SI Appendix*, Table S1.

whereas the CAM receptor activates G$_s$ and AC spontaneously (17). Basal BRET between both CIM 5-HT$_7$ receptors and G$_s$ was significantly increased compared with wild-type (WT) 5-HT$_7$, and ligand-induced changes in BRET were abolished. In contrast, basal BRET between the CAM 5-HT$_7$ receptor and G$_s$ was significantly decreased compared with WT 5-HT$_7$, and the agonist-induced decrease was occluded (Fig. 2 *B* and *C*). These results suggested that CIM 5-HT$_7$ receptors should efficiently sequester G$_s$ heterotrimers, whereas CAM 5-HT$_7$ should activate G$_s$. As expected, CIM 5-HT$_7$ receptors completely prevented β$_2$AR-mediated activation of AC, whereas CAM 5-HT$_7$ constitutively activated AC (Fig. 2*D*). We also found that expression of CIM 5-HT$_7$ significantly inhibited the ability of forskolin to activate AC (*SI Appendix*, Fig. S2). A similar effect has been described for inverse-agonist–bound 5-HT$_7$ receptors (18), although the underlying mechanism is unclear. Forskolin binds directly to AC, but its actions are highly synergistic with Gα$_s$ (19, 20), and G$_s$ is required for potent forskolin-induced AC activation in HEK 293 cells (21, 22). Therefore, inhibition of forskolin action is consistent with efficient sequestration of G$_s$ heterotrimers by inactive 5-HT$_7$ receptors.

We then assessed the relative stability of inactive- and active-state 5-HT$_7$–G$_s$ complexes with a competition experiment in which BRET between 5-HT$_7$ and G$_s$ was monitored during activation of unlabeled β$_2$AR (Fig. 2*E*). This experiment was carried out in the absence of nucleotides to enable efficient recruitment of G$_s$ heterotrimers by active β$_2$AR. In the presence of MT, β$_2$AR activation caused a biphasic decrease in BRET between 5-HT$_7$ and G$_s$ (k_{fast} = ~0.2 s^{-1}; k_{slow} = ~0.03 s^{-1}; 48% fast) (*SI Appendix*, Table S1), consistent with a transient association of inactive 5-HT$_7$ and G$_s$ under these conditions. However, in the presence of 5-HT, β$_2$AR activation caused an even more rapid decrease in BRET between 5-HT$_7$ and G$_s$ (k_{fast} = ~0.5 s^{-1}; k_{slow} = ~0.03 s^{-1}; 83% fast). This rapid decrease started from a lower baseline due to 5-HT–induced dissociation of inactive-state complexes, but nonetheless demonstrates the existence of active-state 5-HT$_7$–G$_s$ complexes in the presence of 5-HT. Similar kinetic results were obtained with CIM and CAM 5-HT$_7$ mutants (*SI Appendix*, Table S1). These results suggest that even in the absence of nucleotides, inactive-state 5-HT$_7$–G$_s$ complexes are more stable than active-state 5-HT$_7$–G$_s$ complexes in cell membranes, and are consistent with agonist-induced net dissociation under the same conditions (Fig. 1*E*).

5-HT$_7$ Readily Adopts the Active State. We next examined the interaction of 5-HT$_7$ receptors with mini G$_s$ (mGs) proteins, as these engineered Gα subunits were designed to stabilize the active state of G$_s$-coupled GPCRs (23). We found that unliganded 5-HT$_7$ receptors spontaneously recruited mGs proteins to the plasma membrane, as assessed by both confocal imaging (Fig. 3 *A* and *B*) and BRET assays (Fig. 3*C*). Moreover, 5-HT$_7$ interactions with mGs were only weakly sensitive to agonists or inverse agonists but in a manner opposite to that observed with G$_s$ heterotrimers; the association of 5-HT$_7$ and mGs was modestly enhanced by 5-HT and inhibited by MT (Fig. 3*C*). Similar results were obtained in

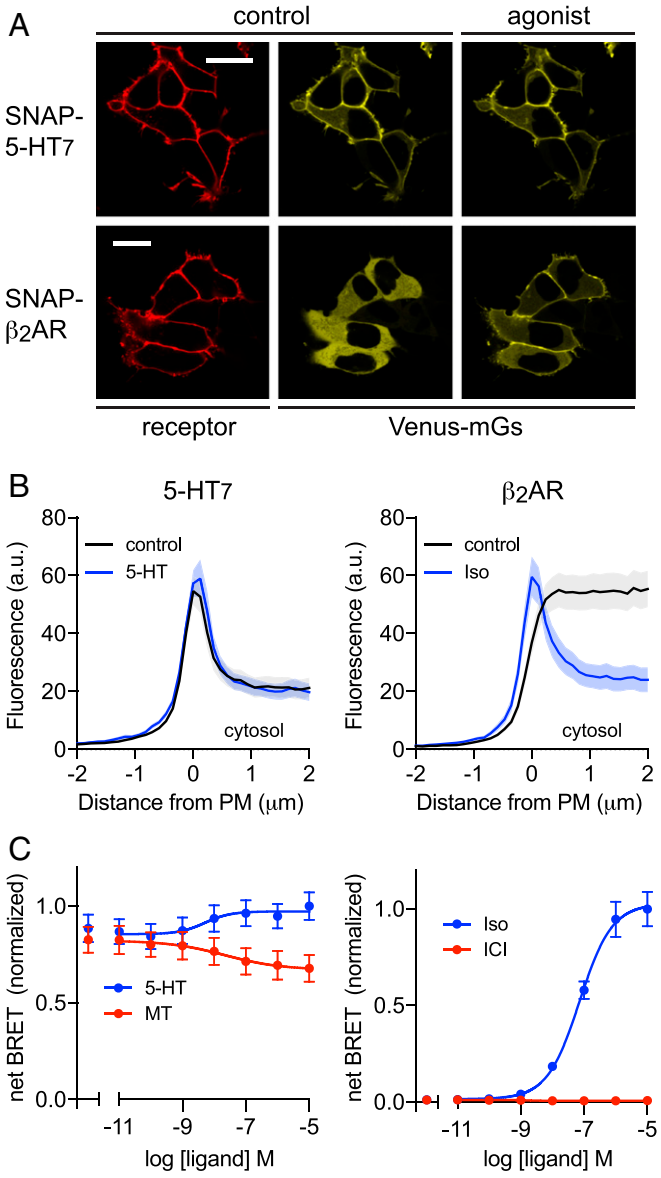

Fig. 3. Unliganded and active 5-HT$_7$ receptors bind mGs proteins. (*A*) Confocal images of cells expressing SNAP-tagged 5-HT$_7$ or β_2AR labeled with BG-649-PEG-biotin and NES-Venus-mGs, before and after the addition of 10 μM 5-HT or isoproterenol. (Scale bars: 20 μm.) (*B*) Line profiles of fluorescence intensity drawn normal to the plasma membrane from experiments as in *A*. Data are mean ± SEM; n = 32–45 cells. (*C*) BRET between Nluc-mGs and the plasma membrane marker Venus-kRas in cells expressing 5-HT$_7$ or β_2AR receptors as a function of agonist or inverse agonist concentration. Data are mean ± SEM; n = 5.

pull-down assays with detergent-solubilized 5-HT$_7$ receptors and mGs (*SI Appendix*, Fig. S1). Consistent with these observations, CIM 5-HT$_7$ receptors lost the ability to interact with mGs, whereas the CAM 5-HT$_7$ receptors retained this ability (*SI Appendix*, Fig. S3). These results suggest that mGs is unable to form complexes with inactive 5-HT$_7$ that are analogous to inactive-state 5-HT$_7$–G$_s$ complexes, whereas active 5-HT$_7$ can form complexes with mGs. Furthermore, spontaneous association with mGs implies that 5-HT$_7$ receptors readily adopt an active state in the absence of an agonist. This was not the case for β_2AR, which required agonist activation for robust association with mGs under similar conditions (Fig. 3 *A*–*C*).

Most GPCRs intrinsically favor inactive conformations (2), and high-affinity agonist binding is usually not evident unless a nucleotide-free G protein (or a G protein surrogate) is present to stabilize the active state. An unusual characteristic of 5-HT$_7$ receptors is a high-affinity agonist binding that persists even in the presence of guanine nucleotides (24–26). This could reflect either stabilization of active 5-HT$_7$ by nucleotide-bound G$_s$ (25) or, alternatively, an intrinsic tendency of the receptor to adopt active states even when G$_s$ is not present. To test these alternatives, we performed [^{3}H]SB269970 competitive binding assays using membranes prepared from gene-edited cells that do not express Gα$_s$ family subunits, with and without the expression of exogenous Gα$_s$. We found that high-affinity agonist binding was maintained even in the complete absence of G$_s$ (Fig. 4*A*) and was unaffected by addition of guanine nucleotides (Fig. 4*B*). As has been described previously (25, 27), we also observed a small population of low-affinity agonist-binding sites, and the fraction of low-affinity sites was modestly larger when G$_s$ was present (~30%) than when G$_s$ was absent (~20%) (*SI Appendix*, Table S2). The affinity of the inverse agonist [^{3}H]SB269970 was slightly higher when G$_s$ was present (Fig. 4*C*). These results are consistent with the suggestion that 5-HT$_7$ receptors readily adopt active states that bind agonist with high affinity even in the absence of G$_s$, and further suggest that G$_s$ may stabilize an inactive state that binds agonists with low affinity.

Because most GPCRs intrinsically favor inactive conformations, the pharmacologic properties of receptors in the absence of nucleotide-free G proteins or surrogates are thought to reflect primarily the inactive state. Accordingly, agonist-binding affinity under these conditions is relatively low and is only modestly decreased by mutations that inhibit constitutive receptor activity (17), but is significantly increased by mutations that activate constitutive activity (28). However, we found that the CIM 5-HT$_7$ F336R displayed >10,000-fold lower agonist-binding affinity than WT 5-HT$_7$ receptors (Fig. 4*D*). In contrast, the CAM 5-HT$_7$ L173A displayed agonist binding similar to the high-affinity binding component of WT 5-HT$_7$ receptors (Fig. 4*D* and *SI Appendix*, Table S3). As expected, inverse-agonist–binding affinity was higher for CIM 5-HT$_7$ receptors than for CAM 5-HT$_7$ receptors (Fig. 4*E*). Therefore, inactive mutant 5-HT$_7$ receptors that bind G$_s$ tightly bind 5-HT with low affinity, whereas active mutant 5-HT$_7$ receptors that bind G$_s$ weakly bind 5-HT with high affinity. These results are consistent with a negative allosteric interaction between agonist and G$_s$ binding to WT 5-HT$_7$ receptors and a net dissociation of 5-HT$_7$–G$_s$ complexes on agonist binding.

Inactive-State 5-HT$_7$–G$_s$ Complexes Prevent Constitutive Signaling. The foregoing results suggested that inactive- and active-state 5-HT$_7$ receptors form distinct complexes with G$_s$ heterotrimers. Because the C terminus of the Gα subunit is required for active-state GPCR-G protein complexes (29), we guessed that by altering this region, it might be possible to prevent formation of active-state complexes without impairing inactive-state complexes. However, removing a single amino acid from the distal C terminus of Gα$_s$ (Gα$_s$ Δ1) decreased the basal BRET between 5-HT$_7$ and G$_s$, which partially occluded the agonist-induced decrease and enhanced the inverse agonist-induced increase (Fig. 5 *A* and *B* and *SI Appendix*, Fig. S4 *A* and *B*). Removing two amino acids (Gα$_s$ Δ2) reduced the basal BRET to background levels and converted the agonist-induced decrease observed in the presence of apyrase into an increase, implying net receptor-G protein association. Therefore, truncation of the Gα$_s$ C terminus was in fact more effective at disrupting inactive-state 5-HT$_7$–G$_s$ complexes and left active-state complexes at least partially intact. By comparison, the same truncations had no effect on the basal BRET between β_2AR and G$_s$ (Fig. 5*C*) and progressively inhibited agonist-induced coupling of β_2AR to G$_s$ (Fig. 5*D* and *SI Appendix*, Fig. S4 *C* and

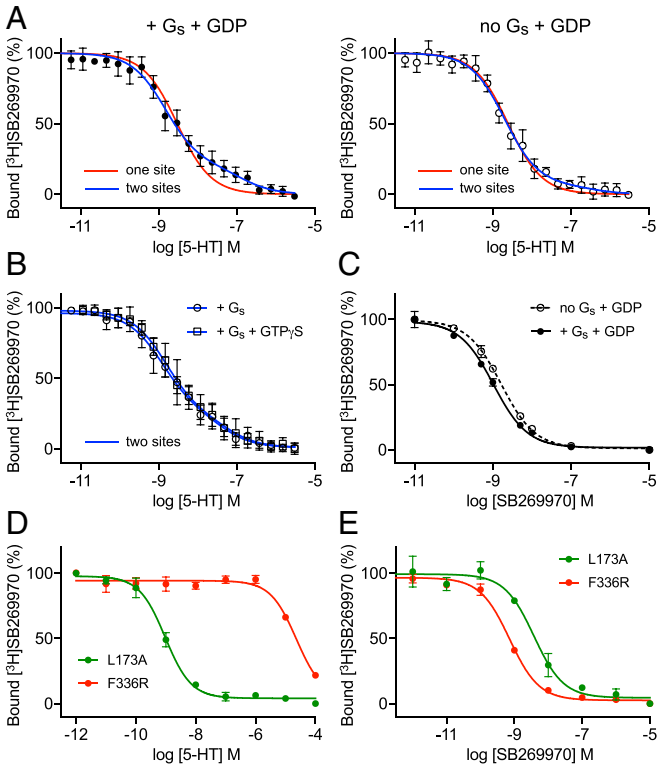

Fig. 4. High-affinity agonist binding to 5-HT$_7$ does not require G$_s$. (*A*) Competitive binding assays between the inverse agonist [^{3}H]SB269970 and 5-HT using membranes prepared from cells lacking endogenous Gα$_s$ subunits, with or without coexpression of exogenous Gα$_s$ in the presence of 100 μM GDP. Data are mean ± SD; n = 6 to 9. Least squares fits to one- and two-site binding models are superimposed. (*B*) As in *A* but with coexpression of Gα$_s$ and in the presence of no added nucleotide or 100 μM GTPγS. Data are mean ± SD; n = 6 to 9. (*C*) Homologous competitive binding with unlabeled SB269970 with or without expression of Gα$_s$. Data are mean ± SEM; n = 3. (*D*) Agonist binding to the activated mutant 5-HT$_7$ L173A is similar to high-affinity binding to WT 5-HT$_7$, whereas agonist binding to the inactive mutant 5-HT$_7$ F336R is severely impaired. Data are mean ± SEM; n = 3. (*E*) Inverse agonist binds to the inactive mutant 5-HT$_7$ F336R with higher affinity than for the active L173A mutant. Data are mean ± SEM; n = 3. Grouped data from all radioligand-binding experiments are provided in *SI Appendix*, Tables S2–S4.

D), again suggesting that these receptors form only active-state complexes with G$_s$.

Because the last two amino acids of Gα$_s$ are leucine residues, we suspected that hydrophobicity in this region was necessary for the inactive-state interaction with 5-HT$_7$. Consistent with this notion, mutation of the last amino acid (Leu394) to isoleucine preserved the behavior of WT Gα$_s$, whereas mutations of Leu394 to polar residues (Gln, Arg, or Glu) virtually abolished the inactive-state interaction with 5-HT$_7$ (*SI Appendix*, Figs. S5 and S6). Gα$_s$ Leu394Ile also interacted with β$_2$AR normally, whereas Leu394Gln, Leu394Arg, and Leu394Glu showed modest impairment of agonist-induced coupling comparable to that observed with truncated Gα$_s$ (*SI Appendix*, Figs. S5 and S6).

During these experiments, we noticed that nucleotide depletion with apyrase significantly enhanced the basal BRET (when no ligand was present) between 5-HT$_7$ and G$_s$ when Gα$_s$ subunits were truncated; nucleotide sensitivity peaked at Gα$_s$ Δ2 and declined back to baseline (WT) by Gα$_s$ Δ4 (Fig. 5*E*). This was not observed with β$_2$AR (Fig. 5*F*), suggesting that 5-HT$_7$ (but not β$_2$AR) was spontaneously forming active-state complexes with truncated nucleotide-free heterotrimers. This in turn implied that 5-HT$_7$ should constitutively activate truncated mutants. Indeed, in cells expressing 5-HT$_7$, basal cAMP levels increased when Gα$_s$ was truncated, peaking at Gα$_s$ Δ2 and declining back to baseline by Gα$_s$ Δ4 (Fig. 5*G*). Stimulation with 5-HT produced only modest further increases in cAMP when Gα$_s$ was truncated, even though the AC activator forskolin could produce large further increases (Fig. 5*G* and *SI Appendix*, Fig. S7). These trends were not due to changes in spontaneous nucleotide release or hydrolysis, as truncation of Gα$_s$ progressively inhibited basal and agonist-stimulated cAMP accumulation mediated by β$_2$AR receptors (Fig. 5*H*), mirroring the progressive impairment seen in direct coupling assays. 5-HT$_7$ (but not β$_2$AR) also constitutively activated heterotrimers with polar residues in position 394 of Gα$_s$, and agonist-induced activation was occluded (*SI Appendix*, Fig. S5). Therefore, 5-HT$_7$ receptors constitutively activated G$_s$ heterotrimers with which they were unable to form inactive-state complexes, again consistent with a tendency of these receptors to adopt active conformations even when not bound by agonist.

Discussion

Taken together, our results support a model wherein agonist binding to 5-HT$_7$ receptors is linked to G$_s$ activation in a manner distinct from conventional GPCR-G protein coupling (Fig. 6*A*). We propose a model wherein 5-HT$_7$ receptors in their basal state (R$_n$) reversibly form encounter complexes (R$_n$G) with G$_s$ heterotrimers. R$_n$G encounter complexes can transition to conventional active-state complexes (R$_a$G) but are more likely to transition to inactive-state complexes (R$_i$G), a process we term "inverse coupling." Constitutive G$_s$ activation occurs through the R$_a$G coupling pathway but is kept in check by accumulation of R$_i$G. Agonist binding does not change the rates governing the formation of R$_n$G encounter complexes or R$_a$G active-state complexes, but does decrease the accumulation of R$_i$G complexes. This decreases the net 5-HT$_7$–G$_s$ association and allows for increased formation of R$_a$G and G$_s$ activation. Our data suggest that the conformational transitions between R$_n$G and R$_i$G are sensitive to agonist binding to the receptor but less sensitive to nucleotide binding to G$_s$, whereas the conformational transitions between R$_n$G and R$_a$G are sensitive to nucleotide binding to G$_s$ but less sensitive to agonist binding to the receptor. If the R$_n$G-to-R$_i$G pathway is blocked (e.g., by truncation or mutation of G$_s$), R$_a$G complexes form spontaneously even in the absence of agonist, because the basal state of 5-HT$_7$ intrinsically favors active conformations (R$_n$ ~ R$_a$). In contrast, conventional GPCRs in their basal state intrinsically favor inactive conformations (R$_n$ ~ R$_i$), but R$_i$G complexes do not form or accumulate (Fig. 6*A*). Conventional R$_n$G encounter complexes either dissociate or progress to R$_a$G, and conformational transitions between R$_n$G and R$_a$G are sensitive to both agonist binding to the receptor and nucleotide binding to the G protein.

Based on these general principles, we defined a set of ordinary differential equations to construct deterministic models of conventional and inverse coupling (*SI Appendix*, Table S5). Simulations based on these models recapitulated the essential features of receptor-G protein association, dissociation, and activation that we observed for β$_2$AR and 5-HT$_7$ receptors. Specifically, agonist binding led to a net association of β$_2$AR and G$_s$ and a net dissociation of 5-HT$_7$ and G$_s$ in either the presence or absence of guanine nucleotides, but increased formation of R$_a$G (and thus G$_s$-GTP) in intact cells (Fig. 6*B*). Notably, our inverse coupling model also predicts that increasing 5-HT$_7$ receptor density will not lead to higher potency signaling; that is, a receptor reserve will not be apparent (Fig. 6*C*). The absence of a receptor reserve has been observed experimentally for 5-HT$_7$ (11), and several studies have reported lower agonist potency than expected based on agonist-binding affinity (9, 11, 27, 30). Our model suggests that this anomalous property of 5-HT$_7$ receptors reflects sequestration of G$_s$ heterotrimers in R$_i$G

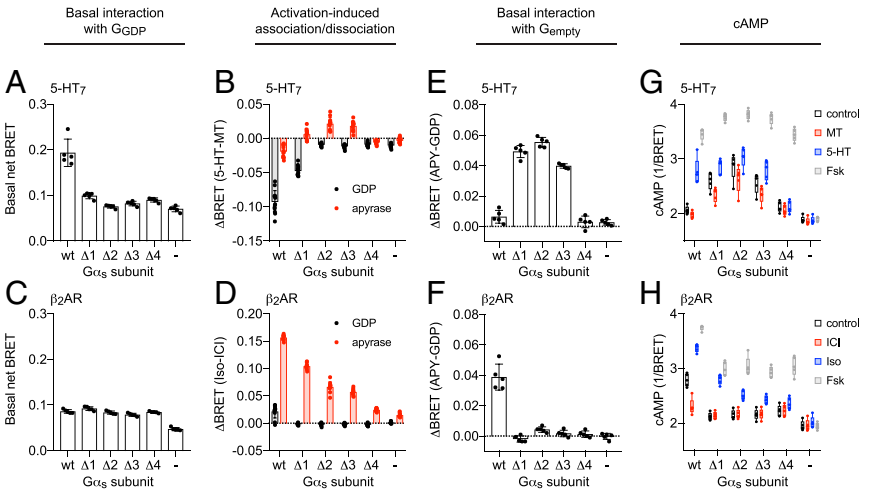

Fig. 5. Truncation of the $G\alpha_s$ C terminus disrupts inactive-state 5-HT_7-G_s complexes and leads to constitutive activation of AC. (*A*) Basal BRET between 5-HT_7-Rluc8 and $G\alpha_s\beta\gamma$-Venus in the presence of GDP decreases as the $G\alpha_s$ C terminus is truncated by one to four amino acids (Δ1–Δ4) or when no Gα (–) is expressed ($n = 5$). (*B*) Agonist-induced decreases in BRET between 5-HT_7-Rluc8 and $G\alpha_s\beta\gamma$-Venus are occluded when $G\alpha_s$ is truncated; ΔBRET(5-HT-MT) is BRET in 5-HT minus BRET in MT ($n = 13$). (*C*) Basal BRET between β_2AR-Rluc8 and $G\alpha_s\beta\gamma$-Venus does not change when $G\alpha_s$ is truncated ($n = 5$). (*D*) Agonist-induced increases in BRET between β_2AR-Rluc8 and $G\alpha_s\beta\gamma$-Venus are diminished when $G\alpha_s$ is truncated. ΔBRET(Iso-ICI) is BRET with isoproterenol minus BRET with ICI-118,551 ($n = 11$). (*E*) Nucleotide-sensitive BRET between 5-HT_7-Rluc8 and $G\alpha_s\beta\gamma$-Venus increases when $G\alpha_s$ is truncated ($n = 5$). (*F*) Nucleotide-sensitive BRET (basal BRET with apyrase minus basal BRET with GDP) between β_2AR-Rluc8 and $G\alpha_s\beta\gamma$-Venus decreases when $G\alpha_s$ is truncated ($n = 5$). Experiments in *A*–*F* were performed in permeabilized cells in the presence of GDP (100 μM) or apyrase. Data are mean ± SD. (*G*) Basal cAMP (control) increases in cells expressing 5-HT_7 receptors when $G\alpha_s$ is truncated, occluding 5-HT–induced cAMP responses ($n = 5$). In all groups, cAMP was further increased by forskolin (Fsk), indicating that the sensor was not saturated. (*H*) Basal cAMP and Iso-induced cAMP responses decrease in cells expressing β_2AR receptors when $G\alpha_s$ is truncated ($n = 5$). In *G* and *H*, boxes represent the 25th to 75th percentiles, whiskers indicate the maximum and minimum, and individual data points are superimposed. All experiments were carried out using cells lacking endogenous $G\alpha_s$ subunits.

complexes when agonist concentrations are below the level at which receptors are saturated.

Our model predicts that G_s heterotrimers should decrease agonist-binding affinity at 5-HT_7 receptors by stabilizing the inactive receptor state. Although we and others have observed a small population of low-affinity agonist-binding sites (25, 27), this fraction was only modestly increased when G_s was present (Fig. 4*A*). It is possible that negative allostery between agonist and G_s binding is difficult to observe in equilibrium-binding experiments due to the transient nature of inactive-state 5-HT_7–G_s complexes (Fig. 2*E*), as well as possible loss of G_s from membrane preparations. A similar problem exists for some active-state GPCR-G protein complexes, as high-affinity agonist binding can be difficult to detect for some receptors in some expression systems (31). Strategies that have been successful in stabilizing active-state complexes for ligand-binding experiments (32) may eventually be able to reveal more robust G_s-mediated inhibition of agonist binding to 5-HT_7 receptors.

In summary, our present results explain several unusual biophysical and pharmacologic properties of 5-HT_7 receptors. We propose that this receptor intrinsically favors active conformations but avoids unrestrained activation of G_s heterotrimers by forming inactive-state 5-HT_7–G_s complexes. Agonist binding acts primarily to prevent the formation of unproductive 5-HT_7–G_s complexes, which indirectly promotes the formation of productive complexes. Thus, a negative allosteric interaction between agonist binding and G_s association is necessary for agonist-induced 5-HT_7 signaling. Recent studies have shown that the allosteric range of GPCRs is broader than previously anticipated (33). Engineered antibodies can stabilize both active and inactive receptor conformations (33–35), and the basal state (R_n in our model) represents a time-weighted average of conformational sampling. Our results suggest that G proteins can also act to stabilize both active and inactive receptor conformations and cooperate with agonist binding in both a positive and a negative manner. Although our results indicate that the distal C terminus of $G\alpha_s$ is required for inactive-state 5-HT_7–G_s complexes, further studies are needed to establish the structural mechanism through which G_s stabilizes the inactive state of the receptor. It will be interesting to determine whether G_s acts in a manner similar to the way in which negative allosteric antibodies stabilize inactive GPCRs (33–35). Several other GPCRs are thought to interact with G proteins before agonist binding (4–8); therefore, it seems possible that inverse coupling will prove to be a conserved mechanism for regulating the sensitivity and dynamic range of cell signaling.

Materials and Methods

Materials. Trypsin, DPBS, PBS, FBS, MEM, DMEM, penicillin/streptomycin, and L-glutamine were obtained from Thermo Fisher Scientific. Receptor ligands (5-HT, isoproterenol, ICI-118,551, and MT) and forskolin were purchased from Cayman Chemical or MilliporeSigma. Detergents (n-dodecyl-β-D-maltoside [DDM] and cholesteryl hemisuccinate [CHS]) were obtained from Anatrace. Digitonin, apyrase, GDPβS, and GDP were purchased from MilliporeSigma or BioBasic. [^{3}H]SB269970 was obtained from PerkinElmer, and polyethylenimine (PEI) MAX was purchased from Polysciences.

Plasmid DNA Constructs. 5-HT_7-Rluc8 was made by amplifying the human 5-HT_7 coding sequence (splice variant d) using the PCR results for 5-HT_7–Tango (36) (Roth Lab PRESTO-Tango Kit; Addgene) and ligating into pRluc8-N1 with HindIII and KpnI. Inactivating and activating mutations were introduced into 5-HT_7–Rluc8 using the QuikChange Mutagenesis Kit (Agilent Technologies) and gBlock fragments (Integrated DNA Technologies) as primers. Plasmids encoding unlabeled human 5-HT_7, β_2AR, $G\alpha_s$-long, and $G\beta_1$ were purchased from the cDNA Resource Center. Truncated and mutated $G\alpha_s$ subunits were derived from WT $G\alpha_s$-long by amplifying the coding sequence with reverse primers incorporating the desired mutation and ligating the resulting fragment into pcDNA3.1(+) using KpnI and XhoI. A plasmid encoding β_2AR-SmBit was derived from unlabeled β_2AR using the QuikChange Mutagenesis Kit and a gBlock primer. A plasmid encoding 5-HT_7–SmBit was derived from unlabeled 5-HT_7 by standard subcloning into a SmBit vector. A plasmid encoding LgBit-$G\gamma_2$ was kindly provided by Stephen

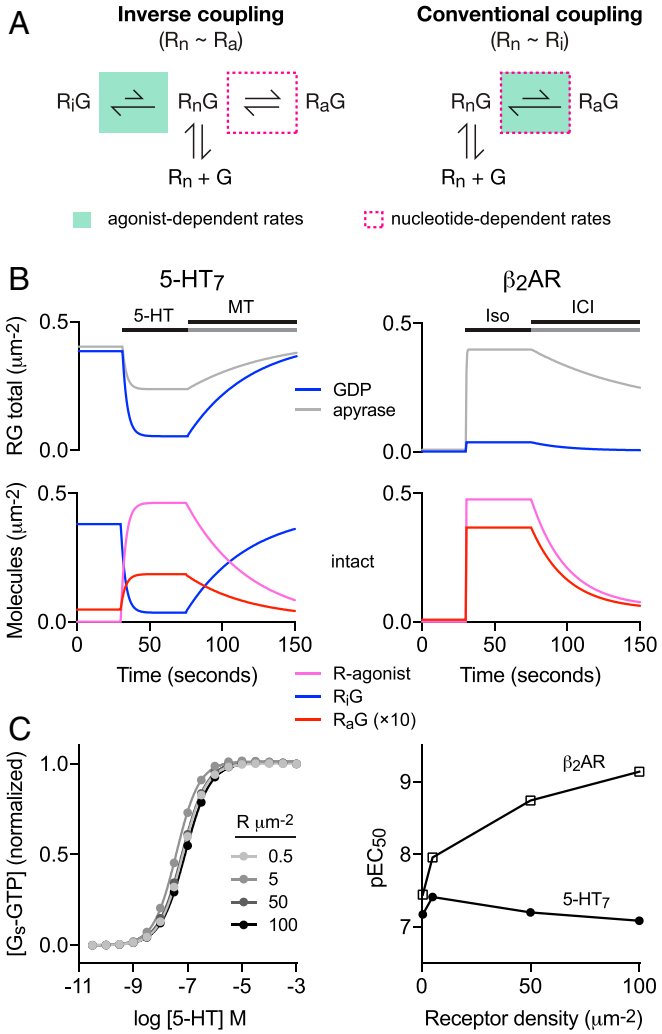

Fig. 6. An inverse coupling model describes the unconventional properties of 5-HT_7 receptors. (*A*) Inverse and conventional coupling models describing the formation of encounter complexes (R_nG), active-state complexes (R_aG), and inactive-state complexes (R_iG). Boxes indicate rates that are influenced by agonist binding to the receptor and nucleotide binding to the G protein. (*B*) Simulations based on ODE models corresponding to *A* recapitulating net dissociation of receptor-G protein complexes for 5-HT_7 but not for β_2AR in response to agonist (*Top*), but increases in R_aG complexes in intact cells for both (*Bottom*). (*C*) Simulated curves plotting normalized [G_s-GTP] vs. [5-HT] across a 200-fold increase in 5-HT_7 expression (*Left*) and plots of simulated pEC_{50} vs. receptor expression for both 5-HT_7 and β_2AR (*Right*). Model parameters and conditions are provided in *SI Appendix*, Table S5.

R. Ikeda, National Institute on Alcohol Abuse and Alcoholism. A plasmid encoding the Nluc-EPAC-VV cAMP sensor was kindly provided by Kirill Martemyanov, The Scripps Research Institute. Plasmids encoding β_2AR-Rluc8, NES-Venus-mGs, NES-Nluc-mGs, Venus-kras, Venus-1–155-Gγ_2, and Venus-155–239-Gβ_1 have been described previously (22, 37, 38). All plasmid constructs were verified by Sanger sequencing.

Cell Culture and Transfection. HEK 293 cells (American Type Culture Collection; CRL-1573) were propagated in plastic flasks and on six-well plates according to the supplier's protocol. HEK 293 cells with targeted deletion of *GNAS* and *GNAL* were a generous gift from Asuka Inoue, Tohoku University, and were derived, authenticated and propagated as described previously (39). Cells were transiently transfected in growth medium using linear PEI MAX (molecular weight 40,000) at a nitrogen/phosphate ratio of 20 and were used for experiments 24 to 48 h later. Up to 3.0 μg of plasmid DNA was transfected in each well of a six-well plate.

BRET and Luminescence Assays. Intact cells were washed twice with 1× DPBS, harvested by trituration, and transferred to opaque black (for BRET) or white (for luminescence) 96-well plates. Permeabilized cells were washed twice with permeabilization buffer (KPS) containing 140 mM KCl, 10 mM NaCl, 1 mM $MgCl_2$, 0.1 mM KEGTA, and 20 mM NaHEPES (pH 7.2); harvested by trituration; permeabilized in KPS buffer containing 10 μg mL^{-1} high-purity digitonin; and then transferred to 96-well plates. Measurements were made from permeabilized cells supplemented with 100 μM GDP, 2 U mL^{-1} apyrase, or apyrase with 100 μM GDPβS. Steady-state BRET and luminescence measurements were performed using a Mithras LB940 photon-counting plate reader (Berthold Technologies). Kinetic BRET and luminescence time course measurements were obtained with a POLARstar Optima plate reader (BMG Labtech). Coelenterazine h (5 μM; Nanolight) or furimazine (NanoGlo; 1:1,000; Promega) were added to all wells immediately before taking measurements with Rluc8 and Nluc, respectively. Raw BRET signals were calculated as the emission intensity at 520 to 545 nm divided by the emission intensity at 475 to 495 nm. Net BRET is the raw BRET ratio minus the ratio measured from cells expressing only the donor.

Confocal Imaging. Cells grown on 25-mm round coverslips were transferred to an imaging chamber and washed with DPBS. Drug solutions were added directly to the chamber by pipetting. Confocal images were acquired using a Leica SP8 scanning confocal microscope with a 63×, 1.4 NA objective. Venus was excited with a 488-nm diode laser and detected at 500 to 650 nm. BG-649–PEG–biotin was excited with a 633-nm diode laser and detected at 640 to 750 nm.

Membrane Preparation and Radioligand Binding. Transfected cells were washed twice with cold PBS/EDTA and resuspended in cold DPBS. After pelleting at 600 × *g* for 10 min at 4 °C, cells were resuspended in cold homogenization buffer containing 75 mM Tris·HCl pH 7.4, 2 mM EDTA, and protease inhibitor mixture (Roche). Cells were sonicated (three 5-s pulses at 20% amplitude with a 50-s cooldown period between each pulse), debris was pelleted at 500 × *g* for 10 min at 4 °C, and supernatants were centrifuged at 50,000 × *g* for 30 min at 4 °C. Pellets were resuspended in assay buffer containing 100 mM NaCl, 10 mM $MgCl_2$, and 20 mM Hepes, pH 7.4, then snap-frozen and stored at −80 °C. Competitive binding assays were performed as described previously (26) by incubating membranes with [^{3}H]SB269970 (2.5 to 2.8 nM) and increasing concentrations of 5-HT in 96-well plates. Plates were incubated at 23 °C for 60 min and then harvested onto UniFilter-96 GF/C microplates (PerkinElmer), presoaked in 0.3% polyethyleneimine (MilliporeSigma) using a universal harvester, and washed three to four times with ∼0.25 mL per well of ice-cold buffer containing 50 mM Tris·HCl pH 7.0 and 2 mM $MgCl_2$. The filters were dried and counted at ∼40% efficiency in a TopCount liquid scintillation counter using 20 μL per well of MicroScint liquid scintillation mixture (PerkinElmer). Alternatively, cell membranes were incubated with 1 nM [^{3}H]SB269970 and various concentrations of 5-HT or unlabeled SB269970 for 3 h at room temperature in binding buffer containing 20 mM Hepes pH 7.5, 50 mM NaCl, 1 mM EDTA, 5 mM $MgCl_2$, and 0.1% (wt/vol) BSA (Fig. 4 *C*–*E*). After incubation, the reaction was terminated by adding cold binding buffer, followed by rapid filtering through glass fiber prefilters using a semiautomated harvester (Brandel). The filters were then washed three times with 5 mL of cold binding buffer and transferred to scintillation vials. Liquid scintillation mixture (5 mL; CytoScint; MP Biomedicals) was added on top of each filter. After overnight incubation, the radioactivity of the filters was measured with a Beckman LS6500 scintillation counter.

Pull-Down Assays. HEK 293 cells were transiently transfected with Nluc-Gγ_2, Gβ_1, Gα_s-long, and either SNAPf-β_2AR or SNAPf-5HT_7 in a 1:1:2:1 ratio or Nluc-mGs and either SNAPf-β_2AR or SNAPf-5HT_7 in a 2:1 ratio. After 48 h, cells were incubated with 100 nM BG-649-PEG-biotin dye (New England BioLabs) in complete growth medium for 1 h at 37 °C. After three washes with DPBS, membranes were prepared as above, with the addition of 10 μM GDP and receptor ligands (10 μM 5-HT, MT, isoproterenol, or ICI-118,551) to the homogenization buffer. Membranes were solubilized in 500 μL of solubilization buffer (20 mM Hepes pH 7.8, 150 mM NaCl, 2 mM $MgCl_2$, 20% [vol/vol] glycerol, 1% [wt/vol] DDM, 0.2% [wt/vol] CHS, and protease inhibitor mixture [Roche]), 100 μM GDP or 2 U mL^{-1} apyrase, and receptor ligands as above for 3 h at 4 °C with gentle rotation. Solubilized membranes were incubated with 250 μg of streptavidin (sAV) beads (Dynabeads MyOne sAV C1; Thermo Fisher Scientific) that had been washed with wash buffer (20 mM Hepes pH 7.8, 100 mM NaCl, 2 mM $MgCl_2$, 10% [vol/vol] glycerol, 0.1% [wt/vol] DDM, 0.02% [wt/vol] CHS, and protease inhibitor mixture) for 2.5 h at 4 °C with gentle rotation. Beads were washed five times with 1 mL of wash buffer supplemented with either 50 μM GDP or 1 U mL^{-1} apyrase and

receptor ligands, diluted in 500 μL of working solution (20 mM Hepes pH 7.8, 100 mM NaCl, 2 mM $MgCl_2$, 0.1% [wt/vol] DDM, and 0.02% [wt/vol] CHS) and transferred to opaque black 96-well plates. BG-PEG-SNAP-649 fluorescence was determined using a Synergy Neo2 plate reader (BioTek; excitation, 640 nm; emission, 676 nm). Furimazine (NanoGlo, 1:1,000; Promega) was added, and luminescence was measured without wavelength selection. Recovered Nluc activity (G_s or mGs) was normalized to fluorescence (receptor).

Computational Modeling. Rule-based deterministic models of conventional and inverse coupling based on ordinary differential equations (ODE) were constructed using the Virtual Cell (VCell) modeling platform (40, 41). Initial reactions and parameters followed a previously published analytical model (42), which was modified to include three receptor states, R_iG complexes (for the inverse coupling model only), and inverse agonist binding. Both models included basal (R_n), inactive (R_i), and active (R_a) receptor states, each of which could bind reversibly to agonist (L_a) or inverse agonist (L_i). G proteins could be empty, bound to GDP, or bound to GTP and could bind reversibly to ligand-bound or unbound receptors. Reactions, parameters, and initial conditions are given in *SI Appendix*, Table S5). The VCell, "5HT7_Jang_2020" by user "wojang," can be accessed within the VCell software (available at https://vcell.org).

Statistical Testing. Hypothesis tests were carried out with the two-tailed paired *t* test, one-sample *t* test, one-way ANOVA using Dunnett's test for multiple comparisons against a control, or two-way ANOVA using Sidak's test for multiple comparisons, as indicated in figure legends. Replicates were separate cultures of transfected cells derived from the two cell lines used. All data were analyzed using GraphPad Prism.

Data Availability. All study data are included in the main text and *SI Appendix*.

ACKNOWLEDGMENTS. We thank Aska Inoue for providing CRISPR-modified cells lacking $G\alpha_s$ family subunits, and Steve Ikeda, Kirill Martemyanov, and Bryan Roth for providing plasmid DNA. We also thank Najeah Okashah, Qingwen Wan, Alexey Bondar, and Sumin Lu for technical assistance and critical discussion. This study was supported by the NIH (Grants GM130142, to N.A.L. and GM128641, to C.Z.), the Norwegian Council on Cardiovascular Diseases, the South-Eastern Norway Regional Health Authority, the Anders Jahre Foundation for the Promotion of Science, the Simon Fougner Hartmann Family Foundation, the Family Blix Foundation, and the University of Oslo (to F.O.L.).

1. K. L. Pierce, R. T. Premont, R. J. Lefkowitz, Seven-transmembrane receptors. *Nat. Rev. Mol. Cell Biol.* **3**, 639–650 (2002).
2. W. I. Weis, B. K. Kobilka, The molecular basis of G protein-coupled receptor activation. *Annu. Rev. Biochem.* **87**, 897–919 (2018).
3. A. De Lean, J. M. Stadel, R. J. Lefkowitz, A ternary complex model explains the agonist-specific binding properties of the adenylate cyclase-coupled beta-adrenergic receptor. *J. Biol. Chem.* **255**, 7108–7117 (1980).
4. M. Bouaboula *et al*., A selective inverse agonist for central cannabinoid receptor inhibits mitogen-activated protein kinase activation stimulated by insulin or insulin-like growth factor 1. Evidence for a new model of receptor/ligand interactions. *J. Biol. Chem.* **272**, 22330–22339 (1997).
5. F. Monczor *et al*., Tiotidine, a histamine H_2 receptor inverse agonist that binds with high affinity to an inactive G-protein-coupled form of the receptor. Experimental support for the cubic ternary complex model. *Mol. Pharmacol.* **64**, 512–520 (2003).
6. M. Damian *et al*., Ghrelin receptor conformational dynamics regulate the transition from a preassembled to an active receptor:G_q complex. *Proc. Natl. Acad. Sci. U.S.A.* **112**, 1601–1606 (2015).
7. M. B. C. Kilander *et al*., Disheveled regulates precoupling of heterotrimeric G proteins to Frizzled 6. *FASEB J.* **28**, 2293–2305 (2014).
8. J. M. Weiss, P. H. Morgan, M. W. Lutz, T. P. Kenakin, The cubic ternary complex receptor–Occupancy model I. Model description. *J. Theor. Biol.* **178**, 151–167 (1996).
9. R. M. Eglen, J. R. Jasper, D. J. Chang, G. R. Martin, The 5-HT_7 receptor: Orphan found. *Trends Pharmacol. Sci.* **18**, 104–107 (1997).
10. B. L. Roth *et al*., Binding of typical and atypical antipsychotic agents to 5-hydroxytryptamine-6 and 5-hydroxytryptamine-7 receptors. *J. Pharmacol. Exp. Ther.* **268**, 1403–1410 (1994).
11. S. Bruheim, K. A. Krobert, K. W. Andressen, F. O. Levy, Unaltered agonist potency upon inducible 5-$HT_{7(a)}$ but not 5-$HT_{4(b)}$ receptor expression indicates agonist-independent association of 5-$HT_{7(a)}$ receptor and G_s. *Recept. Channels* **9**, 107–116 (2003).
12. K. W. Andressen, J. H. Norum, F. O. Levy, K. A. Krobert, Activation of adenylyl cyclase by endogenous $G(_s)$-coupled receptors in human embryonic kidney 293 cells is attenuated by 5-$HT(_7)$ receptor expression. *Mol. Pharmacol.* **69**, 207–215 (2006).
13. K. W. Andressen *et al*., Related GPCRs couple differently to G_s: Preassociation between G protein and 5-HT_7 serotonin receptor reveals movement of $G\alpha_s$ upon receptor activation. *FASEB J.* **32**, 1059–1069 (2018).
14. C. Galés *et al*., Real-time monitoring of receptor and G-protein interactions in living cells. *Nat. Methods* **2**, 177–184 (2005).
15. A. S. Dixon *et al*., NanoLuc complementation reporter optimized for accurate measurement of protein interactions in cells. *ACS Chem. Biol.* **11**, 400–408 (2016).
16. X. J. Yao *et al*., The effect of ligand efficacy on the formation and stability of a GPCR-G protein complex. *Proc. Natl. Acad. Sci. U.S.A.* **106**, 9501–9506 (2009).
17. Q. Zhou *et al*., Common activation mechanism of class A GPCRs. *eLife* **8**, e50279 (2019).
18. N. Toohey, M. T. Klein, J. Knight, C. Smith, M. Teitler, Human 5-HT_7 receptor-induced inactivation of forskolin-stimulated adenylate cyclase by risperidone, 9-OH-risperidone and other "inactivating antagonists". *Mol. Pharmacol.* **76**, 552–559 (2009).
19. R. K. Sunahara, C. W. Dessauer, R. E. Whisnant, C. Kleuss, A. G. Gilman, Interaction of Gsalpha with the cytosolic domains of mammalian adenylyl cyclase. *J. Biol. Chem.* **272**, 22265–22271 (1997).
20. P. A. Insel, R. S. Ostrom, Forskolin as a tool for examining adenylyl cyclase expression, regulation, and G protein signaling. *Cell. Mol. Neurobiol.* **23**, 305–314 (2003).
21. A. Inoue *et al*., Illuminating G-protein-coupling selectivity of GPCRs. *Cell* **177**, 1933–1947.e25 (2019).
22. N. Okashah *et al*., Variable G protein determinants of GPCR coupling selectivity. *Proc. Natl. Acad. Sci. U.S.A.* **116**, 12054–12059 (2019).
23. R. Nehmé *et al*., Mini-G proteins: Novel tools for studying GPCRs in their active conformation. *PLoS One* **12**, e0175642 (2017).
24. D. R. Thomas *et al*., [$^{(3)}$H]-SB-269970: A selective antagonist radioligand for 5-HT$(_7)$ receptors. *Br. J. Pharmacol.* **130**, 409–417 (2000).
25. G. L. Alberts, C. L. Chio, W. B. Im, Allosteric modulation of the human 5-HT$(_{7A})$ receptor by lipidic amphipathic compounds. *Mol. Pharmacol.* **60**, 1349–1355 (2001).
26. K. A. Krobert, T. Bach, T. Syversveen, A. M. Kvingedal, F. O. Levy, The cloned human 5-HT_7 receptor splice variants: A comparative characterization of their pharmacology, function and distribution. *Naunyn Schmiedebergs Arch. Pharmacol.* **363**, 620–632 (2001).
27. A. H. Ulsund *et al*., Preassociation between the 5-HT_7 serotonin receptor and G protein G_s: Molecular determinants and association with low potency activation of adenylyl cyclase. *FASEB J.* **33**, 3870–3886 (2019).
28. P. Samama, S. Cotecchia, T. Costa, R. J. Lefkowitz, A mutation-induced activated state of the β_2-adrenergic receptor: Extending the ternary complex model. *J. Biol. Chem.* **268**, 4625–4636 (1993).
29. Y. Du *et al*., Assembly of a GPCR-G protein complex. *Cell* **177**, 1232–1242.e11 (2019).
30. J. R. Jasper, A. Kosaka, Z. P. To, D. J. Chang, R. M. Eglen, Cloning, expression and pharmacology of a truncated splice variant of the human 5-HT7 receptor (h5-HT7b). *Br. J. Pharmacol.* **122**, 126–132 (1997).
31. R. Seifert, T. W. Lee, V. T. Lam, B. K. Kobilka, Reconstitution of β_2-adrenoceptor-GTP-binding-protein interaction in Sf9 cells: High coupling efficiency in a β_2-adrenoceptor-G(s α) fusion protein. *Eur. J. Biochem.* **255**, 369–382 (1998).
32. R. Seifert, K. Wenzel-Seifert, B. K. Kobilka, GPCR-galpha fusion proteins: Molecular analysis of receptor-G-protein coupling. *Trends Pharmacol. Sci.* **20**, 383–389 (1999).
33. D. P. Staus *et al*., Allosteric nanobodies reveal the dynamic range and diverse mechanisms of G-protein-coupled receptor activation. *Nature* **535**, 448–452 (2016).
34. T. Hino *et al*., G-protein-coupled receptor inactivation by an allosteric inverse-agonist antibody. *Nature* **482**, 237–240 (2012).
35. T. Che *et al*., Nanobody-enabled monitoring of kappa opioid receptor states. *Nat. Commun.* **11**, 1145 (2020).
36. W. K. Kroeze *et al*., PRESTO-Tango as an open-source resource for interrogation of the druggable human GPCRome. *Nat. Struct. Mol. Biol.* **22**, 362–369 (2015).
37. B. Hollins, S. Kuravi, G. J. Digby, N. A. Lambert, The C terminus of GRK3 indicates rapid dissociation of G protein heterotrimers. *Cell. Signal.* **21**, 1015–1021 (2009).
38. Q. Wan *et al*., Mini G protein probes for active G protein-coupled receptors (GPCRs) in live cells. *J. Biol. Chem.* **293**, 7466–7473 (2018).
39. W. Stallaert *et al*., Purinergic receptor transactivation by the β_2-adrenergic receptor increases intracellular Ca^{2+} in nonexcitable cells. *Mol. Pharmacol.* **91**, 533–544 (2017).
40. J. Schaff, C. C. Fink, B. Slepchenko, J. H. Carson, L. M. Loew, A general computational framework for modeling cellular structure and function. *Biophys. J.* **73**, 1135–1146 (1997).
41. M. L. Blinov *et al*., Compartmental and spatial rule-based modeling with Virtual Cell. *Biophys. J.* **113**, 1365–1372 (2017).
42. T. Sungkaworn *et al*., Single-molecule imaging reveals receptor-G protein interactions at cell surface hot spots. *Nature* **550**, 543–547 (2017).